SHEAR STRENGTH OF MASONRY PIERS

by D. Benedetti[I] and M.L. Casella [II]

SUMMARY

Shear tests on brick masonry piers are presented and different interpretative schemes of failure discussed.

INTRODUCTION

Design problems arising from the strengthening and the repairing of masonry buildings need reliable criteria to predict the ultimate strength of piers under lateral loads. For this purpose a number of approximate formulas expressing ultimate shear as a function of material characteristics and external loading already exist. All these formulas are of experimental origin and differ from one another. This is because the tests they were based on also differed in the ways they reproduced the actual boundary conditions of shear wall piers. Some criteria are based on the ultimate stress theory, i.e. they consider failure to occur when the tensile strength of the material is exceeded by the positive principal stress in a significant point of the panel, generally in its central point. The inherent assumption of this procedure is that failure is practically coincident with the first appearance of cracks in the central point of the panel; note however that in many instances some lateral resistance can still be developed after the first crackings.

Principal tensile stresses are worked out on the basis of simplified hypotheses on the state of stress existing at the chosen point; these hypotheses are different from one another in various criteria. A common assumption is to consider the panel to be of a homogeneous and isotropic material. Although this is evidently not the case for masonry, good agreement with experimental results is generally found. This is due to the fact that the difference between the real and the assumed material and state of stress is somehow annulled by the value of the tensile strength derived within each failure hypothesis. It follows that if experimental results are interpreted by means of a given hypothesis using the appropriate tensile strength only small discrepancies arise between the predicted and the experimental values of lateral resistance. So: (1) the values of tensile strength found for a given material through the interpretation of experimental results differ from one another and must be seen as conventional values, characteristic of the given criteria and not of the material; (2) these values cannot be taken to describe local failure envelopes in a homogeneous equivalent material, for instance for the use in computer programs.

Tests carried out to evaluate the shear strength of brick masonry panels will be presented in this paper. The tests were performed by means of experimental equipment checked to represent the actual boundary conditions of a real pier. The results can contribute to a discussion on some of the topics already mentioned i.e.: (1) the postcracking behaviour of panels, (2) comparison of the nominal tensile strength derived by different criteria, (3) assessment of the possibility to use these values to define local

(I) Associate Professor, Dept. of Structural Engineering, Technical University of Milan, Italy.

(II) Associate Researcher, C.I.S.M., Udine, Italy.

strength envelopes.

TEST EQUIPMENT

The loading apparatus was designed to reproduce the working conditions of a pier. A finite elements analysis carried out on masonry shear walls by the non-linear code ADINA [1] showed that two phases of pier behaviour can be identified. The analysis was carried out on homogeneous material with the local failure envelope of Fig.15 . The first phase occurs in the elastic stage during which the pier's rotational equilibrium is due to moments arising on the two bases of the panel (Fig. 1a). The second phase characterises the diagonal cracking and is generally preceded by horizontal cracks in the tension zones of the pier (Fig. 1b). This has been supported both by results of tests carried out on half-scale models of rural buildings [2] and by inspection of damages to real buildings during earthquakes (see Fig. 2a). In these conditions equilibrium is maintened by a set of additional normal forces as shown in Fig. 2b .

The testing apparatus is shown in Fig.3 . It was designed to keep the two bases parallel as loads increased. This was obtained by means of two sets of rigid tendons placed at the ends of the loading beam (length of tendons 6 m). The horizontal load was applied statically in steps of 640 kg each. Unloading took place after each four steps. The vertical load was given by an oil jack acting on rollers lying over the loading beam. Teflon sheets were placed between rollers and beam. The loading system was analyzed by finite elements in order to assess its capability to reproduce the pier behaviour described above. Results (Fig.4) showed that the state of stress in the test panel before and at cracking accurately reproduced a real wall pier. This was checked under different vertical loads.

The characteristics of the tested panels are reported in Tab.1 ; three types of bricks were used. The pier dimensions were 100 X 100 cm with variable thickness; cement mortar (R_{bK} = 250 kg/cm^2) was laid only in horizontal joints to represent poor quality construction. A r.c. beam was placed above and below the panel to distribute loads: hence the total height was 140 cm. Note that the loading beam of the testing apparatus was not linked to the r.c. beam of the panels, with bases thus defined by the sections between the masonry panel and the r.c. beams.

TEST RESULTS

Table 2 gives the quantities that describe the behaviour of the various panels.

An analysis of these results enables the following comments to be done:

a) Panels of type A and B bricks behave rather similarly, for the same σ_o the values of τ_f and τ_u are very close. This makes it possible to take the two types of panel as if made of the same material.

b) The ultimate strength tends to increase as σ_o increases, but only a little, as can be seen in Fig.5 , which gives the results for models made of hollow bricks. The increase is more evident for solid bricks.

c) As σ_o grows the additional compression σ_T , due to the vertical forces needed for rotational equilibrium, is reduced, and the resultant of the vertical forces moves towards the centre of the cross-section, giving rise to more steeply sloped cracks.

d) After first cracking the pier can still support further load increases

and absorb considerable displacements, as clearly shown by the load-displacement curves. Fig.6 gives one example for model 3.
e) The values of τ_{res} are fairly high, at least 50% of the ultimate strength. It seems reasonable to suggest that they would be smaller for dynamic loads.
f) Two kinds of failure were noticed: (1) along the brick-mortar joints (Fig.7) in some models with no external vertical load, leading to a brittle type of panel behaviour; (2) cracking even across the bricks (Fig.8).
Fig.9 shows in particular the failure of a hollow brick. The mortar, penetrating into the holes, functions like thick nails, leading to shear deformation in the brick.

These various types of behaviour are taken into account in the failure curve of Fig.10 , proposed by Sinha and Hendry [3] . For small values of the vertical compression σ_v failure occurs along the brick-mortar joints, depending on a relation of type $\tau = \tau_o + \mu \sigma_v$. For higher values of σ_v failure can be explained by the ultimate stress theory. Finally, for very high values of σ_v failure depends essentially on friction. In the case of hollow bricks, with behaviour that can more easily be compared to homogeneous material, the interpretation of failure by means of "ultimate stress" type criteria proved suitable. But for solid bricks the results are dealt with better by cohesion-friction type criteria, with a coefficient μ equal to .45 (Fig.11).

FAILURE CRITERIA

As already stated, in panels built with hollow bricks (types A and B) cracks pass through the bricks thus allowing a failure interpretation based on the ultimate stress theory. Three criteria are considered here, namely: (a) Turnsek and Cacovic [4] , (b) Borchelt [5] , (c) Blume [6] . The state of stress assumed to arise in the center of the panel is shown for each in Fig.12 , together with the relationships expressing τ_f as a funtion of the vertical normal stress and the nominal tensile strength. Note that for criteria (a) and (b) the total vertical normal stress due both to external load (σ_o) and to the additional forces (σ_T) is considered. This is unlike the usual applications of these criteria; only (c) directly includes the additional normal stress. The stress pattern in this case was determined from the results of the photoelastic analysis carried out by Frocht [7] .

Tab.3 gives the values of σ_{tr} determined by these three criteria for each panel of type A and B , with and without σ_T . In order to check the criteria against experimental results, in their analytical expressions (Fig.12) the numerical values of the average tensile strengths (quite different from one another) determined by Tab.3 were introduced, thus giving rise to curves of Figs. 13 and 14 . In Fig.13 τ_f is plotted against σ_o while in Fig.14 it is plotted against $(\sigma_o + \sigma_T)$. As can be seen criteria (a) and (b) fit the experimental data well provided the total normal stress $(\sigma_o + \sigma_T)$ is accounted for, whereas less agreement is found if only σ_o is considered. The third of these criteria, (c), is less adequate to represent experimental data obtained with the present testing technique. This discrepancy arises: both criteria (b) and (c) refer to the same testing method (racking test), they only differ in the state of stress assumed in the interpretative scheme. This is the real stress state for (c), but only approximated for (b). Results show that the assumption of the real state of stress in the racking panel to describe the stress pattern in an actual pier leads to overestimating lateral resistance. On the contrary assumption (b), though

it only roughly describes the state of stress in the racking panel, gives results closer to real pier behaviour. The similarity of the results obtained by criteria (a) and (b) can be explained by their similar analytical formulation although they refer to different testing techniques and panel sizes.

LOCAL STRENGTH ENVELOPES

The failure envelope proposed by Kahn and Saugy |8| was considered to assess the possibility of using the values of σ_{tr} given by Tab.3 to describe the equivalent material properties in a f.e. program (see Fig.15). The choice of this envelope is due to the fact that it proved able to describe the shear behaviour of piers |9| . Moreover it is included in an available computer code |1| . The panel and the loading system were simulated as in Fig.4 for different values of the vertical load and by using the average tensile strengths given by Tab.3 . Only when the tensile strength obtained by (a) with the inclusion of the total normal stress ($\sigma_o + \sigma_T$) was used in the simulated model, were the experimental results satisfactorily approximated. The agreement between computed and experimental results was both in the shape of the load-displacement curve and in the values of the first crack and the ultimate shear. As a matter of example consider Fig.16 referring to the simulation of model 1 .

CONCLUDING REMARKS

Experimental results obtained with a testing procedure set up to reproduce actual pier behaviour under lateral forces have been presented. The analysis of the results makes it possible to show the residual strength of piers after first diagonal cracking and to carry out a comparative discussion on failure criteria based on the ultimate stress theory. It was found that it is possible to use the tensile strength obtained by (a) in biaxial state of stress failure criteria. This may have practical consequences as far as the simulation of masonry systems by means of f.e. codes is concerned. The determination of the equivalent material characteristics at failure can be in fact made on the basis of a simple interpretation of shear tests. It was checked that numerical simulations thus carried out represent satisfactorily the overall behaviour of the panel with particular reference to ultimate loads and displacements. Their use is however inadequate to represent local state of stress which are in practice rather complex due to local dishomogeneity and anisotropy. However detailed informations on local state of stress has a relatively slight importance for practical engineering purposes.

ACKNOWLEDGMENTS

This research has been carried out in the frame of C.N.R. - Geodynamics Project - Publ. No.352 .

REFERENCES

1 Bathe, K.J., " Static and Dynamic Non Linear Analysis Using ADINA", MIT Report, 82448/2.

2 Benedetti, D., Casella, M.L., "Il consolidamento antisismico e la riparazione di edifici in muratura di pietrame. Prove sperimentali", Atti del Convegno C.N.R. 1978, Pubbl. N.280 .

3 Sinha, B.P., Hendry, A.W., "Racking Tests on Storey-Height Shear-Wall Structures with Openings, Subjected to Precompression", Designing Engineering and Constructing with Masonry Products, Gulf Publ. Co., Houston, Texas, May 1969.

4 Turnseck, V., Cacovic, F., 1970, "Some Experimental Results on the Strength of Brick Masonry Walls", SIBMAC Proc., Stoke on Trent.

5 Borchelt, J.G., 1970, "Analysis of Brick Walls Subject to Axial Compression and In-Plane Shear", SIBMAC Proc., Stoke on Trent.

6 Blume, T.A., Prolux, J., 1968, "Shear in Grouted Brick Masonry Wall Elements", Western States Clay Products Ass., S. Francisco, Calif.

7 Frocht , M.M., "Recent Advances in Photoelasticity", Transaction, ASME, Vol.55, Sept.-Dec. 1931 .

8 Khan, M.K., Saugy, B., ACI Publ. SP-34, Concrete for Nuclear Reactors.

9 Yokel, F.Y., Fattal, S.G., "Failure Hypothesis for Masonry Shear Walls", Journal of the Structural Division, ASCE, Vol.102, No. ST3, March 1976.

TABLE 1

model	1	2	3	4	5	6	7	8	9	10	11	12
material	A	A	A	A	A	B	B	B	C	C	C	C
thickness [cm]	25	25	25	25	25	25	12	12	12	12	12	25

A = hollow bricks 25x20x20 cm B = hollow bricks 12x25x12 cm
C = solid bricks 12x25x6 cm

TABLE 2

mod.	σ_o	τ_u	τ_f	σ_T	τ_{res}	failure
1	0	4.35	3.40	4.66	3.70	through bricks
2	3.00	5.12	4.60	3.66	3.58	"
3	6.00	5.12	4.60	2.49	4.35	"
4	10.00	5.63	5.35	1.46	4.00	"
5	3.00	5.12	4.35	3.33	3.07	"
6	0	4.35	4.15	6.97		"
7	3.00	4.80	4.32	3.45	2.35	"
8	6.00	5.65	4.80	3.52	3.50	"
9	0	4.26	4.26	3.50	2.13	joint splitting
10	3.00	6.93	6.37	5.32	4.80	"
11	6.00	7.47	6.35	4.80	6.60	through bricks
12	0	6.14	6.14		3.84	joint splitting

All quantities are expressed in Kg/cm^2

$\sigma_o = \frac{N}{A}$ with N=the external normal load
A=area of cross-section of the panel

σ_T = calculated additional compression at first cracking

$\tau_u = \frac{F_u}{A}$ with F_u =the maximum horizontal load carried by the panel

$\tau_f = \frac{F_f}{A}$ with F_f =the horizontal load that provoks the first diagonal crack

$\tau_{res} = \frac{F_{res}}{A}$ with F_{res}=the maximum load carried by the reloaded panel after failure

TABLE 3

Tensile strengths [Kg/cm^2]

mod. / crit.	1	2	3	4	5	6	7	8	mean values
a(σ_0)	5.10	5.56	4.52	4.45	5.20	6.22	5.15	4.80	5.13
a($\sigma_0+\sigma_T$)	3.28	4.33	3.86	4.13	4.09	3.65	4.01	3.87	3.90
b(σ_0)	3.40	3.34	2.49	2.32	3.10	4.15	3.07	2.66	3.06
b($\sigma_0+\sigma_T$)	1.79	2.35	2.01	2.11	2.21	1.94	2.17	2.00	2.07
c	2.49	2.02	0.98	0.31	1.85	3.04	1.83	1.10	1.70

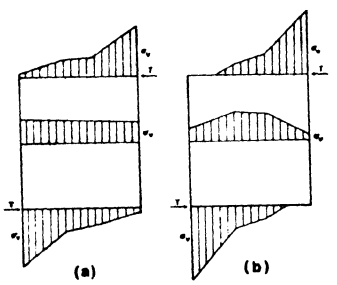

FIG. 1 - Vertical stresses in a pier of a masonry shear wall under lateral and vertical forces, F.e. analysis
(a) linear phase
(b) cracked phase

FIG. 2 - Cracks in an actual pier (a); loading scheme (b)

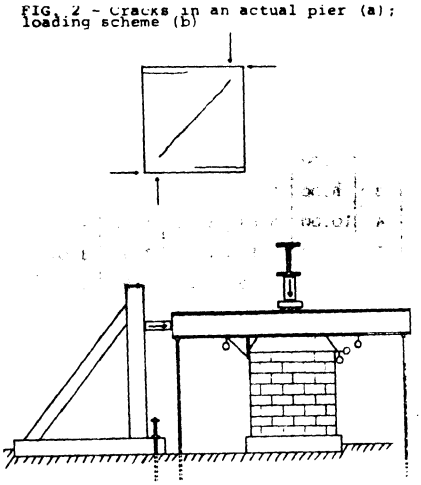

FIG. 3 - Testing apparatus

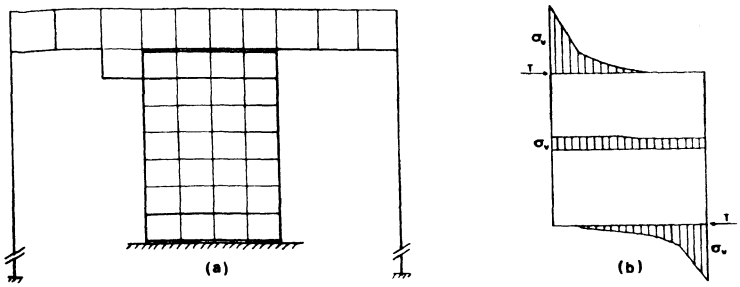

FIG. 4 - F.e. simulation of testing conditions. Mesh (a); vertical stresses on tested panel (b)

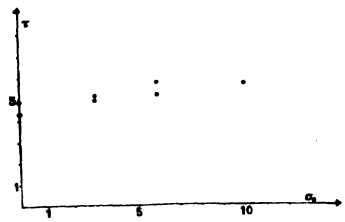

FIG. 5 - Ultimate shear stress against external vertical stress for hollow bricks (stresses in kg/cmq)

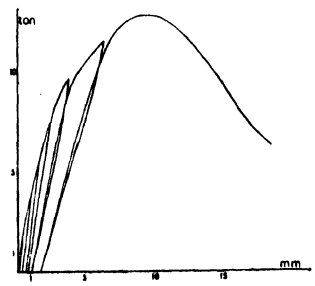

FIG. 6 - Typical load displacement curve

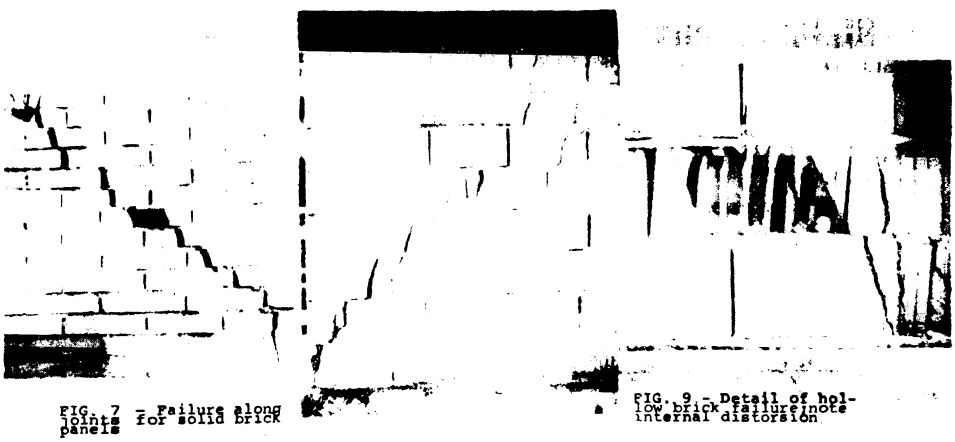

FIG. 7 - Failure along joints for solid brick panels

FIG. 8 - Failure across bricks for hollow brick panels

FIG. 9 - Detail of hollow brick failure:note internal distorsion

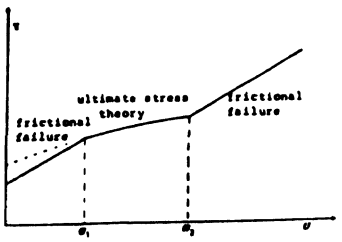

FIG. 10 - Shear failure modes (ref.3)

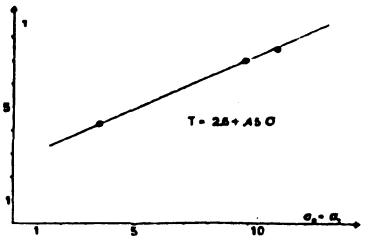

FIG. 11 - Ultimate shear stress against total vertical stress for solid bricks

FIG. 12 - Stress patterns in the central point at first diagonal cracking according to failure criteria (a) ref. 4 (b) ref. 5, (c) ref. 6 σ_o denotes the normal stress due to the external vertical load P. The analytical formulation of criteria (a) and (b) includes σ_T which is neglected in their original formulation

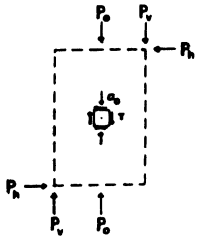

(a)

$\tau = 1.5\ P_h / A$

$\tau_f = \frac{\sigma_{1r}}{1.5}\sqrt{1 + \frac{\sigma_o + \sigma_T}{\sigma_{1r}}}$

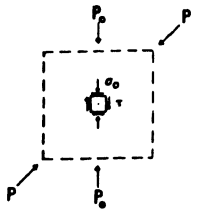

(b)

$\tau = .707\ P/A$

$\tau_f = \sigma_{1r}\sqrt{1 + \frac{\sigma_o + \sigma_T}{\sigma_{1r}}}$

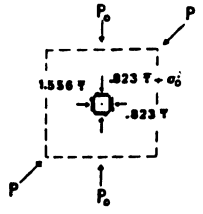

(c)

$\bar{\tau} = .707\ P/A$

$\tau_f = .2365\sigma_o + \sigma_{1r}\left(.473 + .8934\sqrt{1 + \frac{\sigma_o}{\sigma_{1r}} + .07\frac{\sigma_o^2}{\sigma_{1r}^2}}\right)$

FIG. 13 - Shear stress at first diagonal crack against external normal stress (hollow bricks)

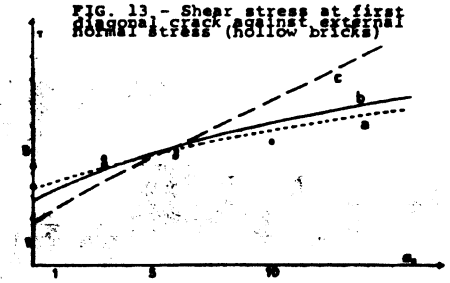

FIG. 14 - Shear stress at first diagonal crack against total normal stress (hollow bricks)

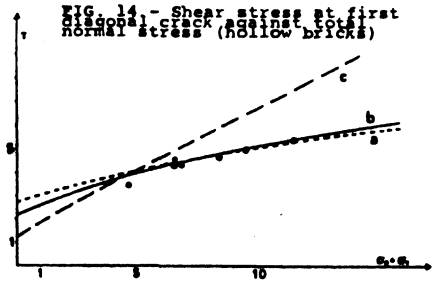

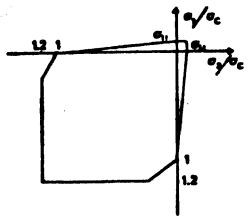

FIG. 15 - Failure envelope (ref.8)

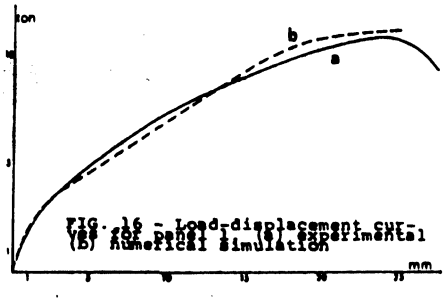

FIG. 16 - Load-displacement curves for panel 1: (a) experimental (b) numerical simulation